37. Bedard K, Krause KH. The NOX family of ROS-generating NADPH oxidases: physiology and pathophysiology. Physiological reviews. 2007; 87: 245–313. PMID: 17237347

38. Liguori L, Andolfo I, de Antonellis P, Aglio V, di Dato V, Marino N, et al. The metallophosphodiesterase Mpped2 impairs tumorigenesis in neuroblastoma. Cell cycle. 2012; 11:569–81. doi: 10.4161/cc.11.3.19063 PMID: 22262177

39. Finn SP, Smyth P, Cahill S, Streck C, O'Regan EM, Flavin R, et al. Expression microarray analysis of papillary thyroid carcinoma and benign thyroid tissue: emphasis on the follicular variant and potential markers of malignancy. Virchows Arch. 2007; 450: 249–60. PMID: 17252232

40. Mazzanti C, Zeiger MA, Costouros NG, Umbricht C, Westra WH, Smith D, et al. Using gene expression profiling to differentiate benign versus malignant thyroid tumors. Cancer Res. 2004; 64: 2898–903. PMID: 15087409

41. Seitz S, Korsching E, Weimer J, Jacobsen A, Arnold N, Meindl A, et al. Genetic background of different cancer cell lines influences the gene set involved in chromosome 8 mediated breast tumor suppression. Genes chromosomes Cancer. 2006; 45: 612–27. PMID: 16552773

42. Wacholder S, Chanock S, Garcia-Closas M, El Ghormli L, Rothman N. Assessing the probability that a positive report is false: an approach for molecular epidemiology studies. J Natl Cancer Inst. 2004; 96: 434–42. PMID: 15026468

Shimizu et al. Arthritis Research & Therapy (2015) 17:223
DOI 10.1186/s13075-015-0751-x

arthritis research&therapy

RESEARCH ARTICLE Open Access

# Effectiveness of imaging modalities for screening IgG4-related dacryoadenitis and sialadenitis (Mikulicz's disease) and for differentiating it from Sjögren's syndrome (SS), with an emphasis on sonography

Mayumi Shimizu[1*], Kazutoshi Okamura[2], Yoshitaka Kise[2,3], Yohei Takeshita[1], Hiroko Furuhashi[2], Warangkana Weerawanich[2], Masafumi Moriyama[4], Yukiko Ohyama[5], Sachiko Furukawa[4], Seiji Nakamura[4] and Kazunori Yoshiura[2]

## Abstract

**Introduction:** The aim of this study was to clarify the effectiveness of various imaging modalities and characteristic imaging features in the screening of IgG4-related dacryoadenitis and sialadenitis (IgG4-DS), and to show the differences in the imaging features between IgG4-DS and Sjögren's syndrome (SS).

**Methods:** Thirty-nine patients with IgG4-DS, 51 with SS and 36 with normal salivary glands were enrolled. Images of the parotid and submandibular glands obtained using sonography, 2-[$^{18}$F]-fluoro-2-deoxy-D-glucose positron emission tomography/computed tomography (FDG-PET/CT), computed tomography (CT) and magnetic resonance imaging (MRI) were retrospectively analyzed. Six oral and maxillofacial radiologists randomly reviewed the arranged image sets under blinded conditions. Each observer scored the confidence rating regarding the presence of the characteristic imaging findings using a 5-grade rating system. After scoring various findings, diagnosis was made as normal, IgG4-DS or SS, considering all findings for each case.

**Results:** On sonography, multiple hypoechoic areas and hyperechoic lines and/or spots in the parotid glands and obscuration of submandibular gland configuration were detected mainly in patients with SS (median scores 4, 4 and 3, respectively). Reticular and nodal patterns were observed primarily in patients with IgG4-DS (median score 5). FDG-PET/CT revealed a tendency for abnormal $^{18}$F-FDG accumulation and swelling of both the parotid and submandibular glands in patients with IgG4-DS, particularly in the submandibular glands. On MRI, SS had a high score regarding the findings of a salt-and-pepper appearance and/or multiple cystic areas in the parotid glands (median score 4.5). Sonography showed the highest values among the four imaging modalities for sensitivity, specificity and accuracy. There were significant differences between sonography and CT ($p = 0.0001$) and between sonography and FDG-PET/CT ($p = 0.0058$) concerning accuracy.

**Conclusions:** Changes in the submandibular glands affected by IgG4-DS could be easily detected using sonography (characteristic bilateral nodal/reticular change) and FDG-PET/CT (abnormal $^{18}$F-FDG accumulation). Even inexperienced observers could detect these findings. In addition, sonography could also differentiate SS. Consequently, we recommend sonography as a modality for the screening of IgG4-DS, because it is easy to use, involves no radiation exposure and is an effective imaging modality.

* Correspondence: shimizu@rad.dent.kyushu-u.ac.jp
[1]Department of Oral and Maxillofacial Radiology, Kyushu University Hospital, 3-1-1 Maidashi, Higashi-ku, Fukuoka 812-8582, Japan
Full list of author information is available at the end of the article

## Introduction

Immunoglobulin G4 (IgG4)-related dacryoadenitis and sialadenitis (IgG4-DS), Mikulicz's disease, has recently been recognized as being an independent entity from Sjögren's syndrome (SS), because of its clinical and serological features [1–3]. Yamamoto et al. [2, 3] stated that these features include persistent gland swelling in IgG4-DS, while gland swelling in SS is periodic. Moreover, salivary function is either normal or improved with the administration of glucocorticoid in IgG4-DS, while it decreases and is not affected by treatment in SS. A further difference is marked elevation of serum IgG4 level in IgG4-DS, while SS show a normal serum IgG4 level. As for anti-SS-A and/or anti-SS-B antibodies, they test negative in IgG4-DS, but have a high positive rate in SS patients. Histopathologically prominent infiltration involving IgG4-positive plasmacytes has been observed using immunostaining in IgG4-DS, while no IgG4-positive plasmacytes have been seen in SS. Additionally, no punctate or globular sialectasis have been observed on sialograms in IgG4-DS, while they are generally observed in SS. Consequently, they considered IgG4-DS to be an entity independent of SS, although it is now known that there are patients who have active disease but normal serum IgG4 levels [4].

Regarding imaging diagnosis of IgG4-DS, most of the studies have been case reports, and we could only find a few which analyzed the effectiveness of the imaging modality involving ≥9 cases as follows: two studies on $^{67}$Ga scintigraphy; two on 2-[$^{18}$F]-fluoro-2-deoxy-D-glucose positron emission tomography/computed tomography (FDG-PET/CT); three on sonography; and two on computed tomography (CT) and magnetic resonance imaging (MRI). Ishii et al. analyzed 13 cases with IgG4-related disease (IgG4-RD) including IgG4-DS using $^{67}$Ga scintigraphy, and showed that there was significant accumulation in the lacrimal glands in seven cases and in the salivary glands in seven cases [5]. In another study, they also found differences in accumulation patterns of $^{67}$Ga between 27 cases of sarcoidosis and 16 cases of IgG4-RD [6]. Some authors have analyzed and verified the usefulness of FDG-PET/CT for staging and follow-up, and have demonstrated abnormal $^{18}$F-FDG uptake in sites involved with IgG4-RD [7, 8]. Some reports have described the characteristic sonographic features of the involved glands, which might be efficient for screening IgG4-DS [9–11]. Sonography is also a useful imaging modality for the follow-up of this disease after corticosteroid therapy [9, 11]. In contrast, CT and MRI have shown enlarged glands with rather nonspecific findings regarding IgG4-DS [12, 13]; although in autoimmune pancreatitis (AIP), one of the IgG4-RD types shows very characteristic findings on both CT and MRI, which has therefore been adopted as one of the diagnostic criteria for AIP [14]. Because these studies have involved only one or two imaging modalities and comparison among modalities are not sufficient, it remains unclear as to which modality is the most efficient in detecting IgG4-DS; the differences in imaging features between IgG4-DS and SS also remain unclear.

The purposes of the present retrospective study were to analyze the imaging features of IgG4-DS using various imaging modalities, and to clarify which imaging modality is the most effective for screening this disease. We also showed the differences in imaging characteristics between IgG4-DS and SS.

## Methods

### Patients

We enrolled 39 patients with IgG4-DS (21 females and 18 males) with a mean age of 59.9 years, between 1999 and 2014. IgG4-DS was serologically and histopathologically confirmed using the following diagnostic criteria: persistent symmetrical swelling involving >2 lacrimal and major salivary glands; an elevated serum level of IgG4 (>135 mg/dl); and infiltration of IgG4-positive plasma cells (percentage of IgG4-positive cells to IgG-positive cells >40 %) on immunostaining [15]. We also analyzed 51 patients with SS (47 females and 4 males) with a mean age of 55.6 years, between 2006 and 2013. SS was diagnosed using both the revised Japanese criteria [16] and the American-European Consensus Group criteria [17]. Additionally, in 2013, 36 patients suffering from oral carcinoma, but with normal salivary glands (14 females and 22 males) with mean age of 63.3 years, were evaluated. This study design was approved by the Ethics Committee of Kyushu University, Japan, and written informed consent was obtained from all of the patients (IRB serial number: 25–287).

### Image preparation

We performed sonography on 30 patients with IgG4-DS, 38 with SS and 36 with normal salivary glands. Sonographic images were taken using a diagnostic unit (Logiq 7: GE Healthcare, Tokyo, Japan) with a center frequency of 12 megahertz (MHz). We extracted B-mode longitudinal images of both the parotid glands (parallel to the retromandibular plane) and the submandibular glands (parallel to the submandibular plane) for this study. Because insufficient Doppler images could be provided for the normal submandibular glands, we only used B-mode images, although we also recorded in the Doppler mode at the time of examination for IgG4-DS and SS. FDG-PET/CT was undertaken in 20 patients with IgG4-DS, 19 with SS and 21 with normal salivary glands. From the superimposed images, where the standardized uptake value (SUV) was reflected as graded colors, we extracted images at the parotid and submandibular gland level, not including the

lacrimal gland level. Similarly, CT images at the parotid and submandibular gland level of 24, 38 and 32 patients with IgG4-DS, SS and normal salivary glands, respectively and MRI of 5, 16 and 19 patients with IgG4-DS, SS and normal salivary glands, respectively, were also extracted for this study. Regarding MRI, besides plain axial T1- and T2-weighted images, we also extracted gadolinium-enhanced T1-weighted images and coronal images of parotid and/or submandibular glands (if any were present). We did not include images of the lacrimal glands. The reasons for this were: 1) we could not undertake sonography of the lacrimal glands for safety reasons regarding the eyes; and 2) when salivary gland tumors were suspected in the patients, lacrimal glands were often not included in the scanning range on CT/MRI.

### Image analysis

Six oral and maxillofacial radiologists (with 2–26 years of diagnostic experience) randomly reviewed the arranged image sets under blinded conditions. The observation order involved sets of: 1) sonographic images; 2) FDG-PET/CT images; 3) CT images; and 4) MRI images. Observations were performed twice with a 3-week interval. Each observer was required to score the confidence rate for the presence of the characteristic imaging findings using a 5-grade rating system (1–5) in the answer sheet as follows: when written characteristic imaging findings were definitely present, 5; when written characteristic imaging findings were definitely absent, 1; presence of a swollen gland, 5; and presence of an atrophied gland, 1. After scoring each finding, diagnosis was made as normal, IgG4-DS or SS, taking into consideration all of the findings for each case.

Figure 1 shows the characteristic findings for IgG4-DS using sonography. They were multiple hypoechoic areas and a reticular pattern on the parotid and submandibular glands, and a nodal pattern on the submandibular glands [9–11]. The characteristic findings for SS were multiple hypoechoic areas, hyperechoic lines and/or spots, and a reticular pattern (a mixture of hypoechoic areas and hyperechoic lines) on both the parotid and submandibular glands [18, 19]. Obscuration of the gland configuration was only assessed in the submandibular glands [19].

On FDG-PET/CT, abnormal $^{18}$F-FDG accumulation in the parotid and submandibular glands was assessed as one of the characteristic findings of IgG4-DS [7, 8] (Fig. 2), when the gland exhibited bright warm colors; red corresponded to an SUV ≥6, orange corresponded to an SUV of around 5, and yellow to bright green corresponded to an SUV of around 4. Gland size was also assessed in the case of both the parotid and submandibular glands.

On CT and MRI (Fig. 2), there are nonspecific findings regarding IgG4-DS [12, 13]. From the images in the references [5, 12, 13] and empirically, we chose parotid and submandibular gland swelling and superficial enhancement of the parotid glands, and the presence of a septum-like structure on the submandibular glands as characteristic CT findings. In relation to characteristic MRI findings, we only chose gland swelling regarding IgG4-DS. In contrast, patients with SS exhibit the following characteristics: atrophic parotid and submandibular glands; heterogeneity of gland parenchyma, which is called a "salt-and-pepper appearance" [20, 21];

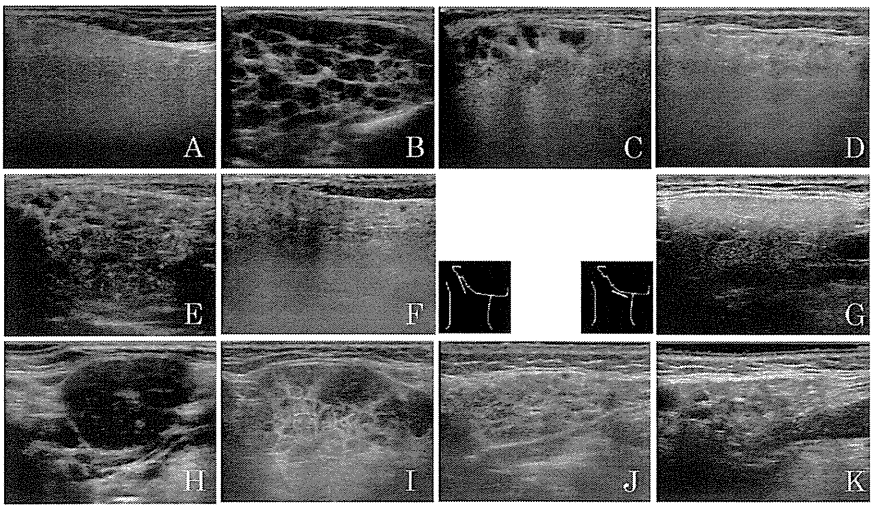


**Fig. 1** Characteristic findings on sonograms. **a** Normal parotid gland. **b-d** Parotid glands of a patient with IgG4-DS. **e, f** Parotid gland of a patient with SS. **g** Normal submandibular gland. **h, i** Submandibular glands of a patient with IgG4-DS. **j, k** Submandibular glands of a patient with SS. Multiple hypoechoic areas (**b-f, i-k**), a reticular pattern (**b, e, i**), and a nodal pattern (**h**) can be seen. Hyperechoic lines and/or spots can also observed (**b-f, i-k**). *IgG4-DS* IgG4-related dacryoadenitis and sialadenitis, *SS* Sjögren's syndrome

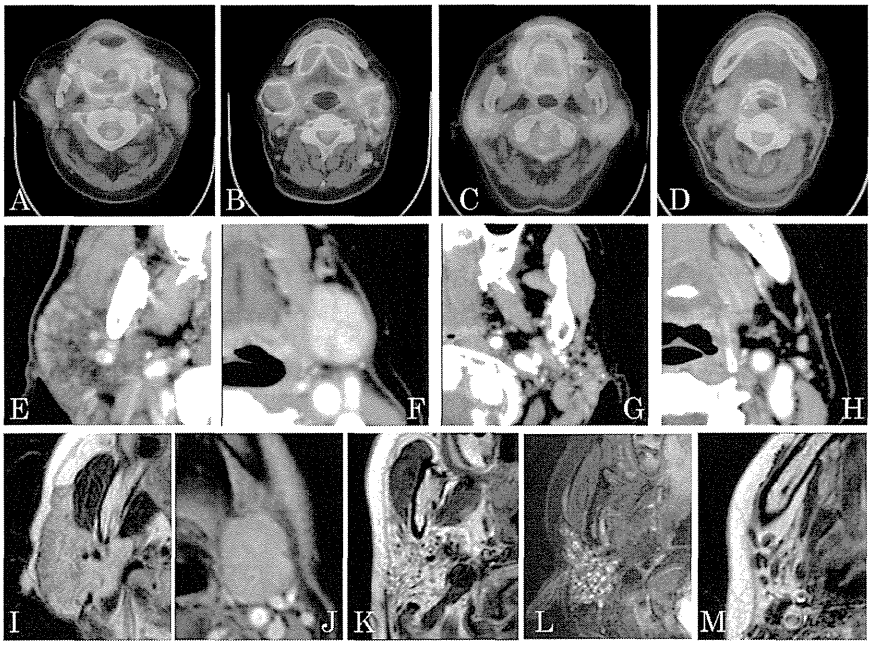


**Fig. 2** Characteristic findings on FDG-PET/CT, CT and MRI. **a-d** FDG-PET/CT, **e-h** CT and **i-m** MRI. **a, e, i** Parotid glands of a patient with IgG4-DS. **b, f, j** Submandibular glands of a patient with IgG4-DS. **c, g, k, l** Parotid glands of a patient with SS. **d, h, m** Submandibular glands of a patient with SS. FDG-PET/CT shows abnormal $^{18}$F-FDG accumulation in the parotid (**a, c**) and submandibular glands (**b**). A patient with IgG4-DS showing parotid (**e, i**) and submandibular gland swelling (**f, j**), superficial enhancement of the parotid glands (**e**), and a septum-like structure in the submandibular glands (**f**). A patient with SS showing atrophic parotid (**g**) and submandibular glands (**h, m**), and a salt-and-pepper appearance (**g, k, l**). It also shows dot-like calcifications on CT (**g**), and small multiple cystic areas on T2-weighted images (**l**). *FDG-PET/CT* 2-[$^{18}$F]-fluoro-2-deoxy-D-glucose positron emission tomography/computed tomography, *CT* computed tomography, *IgG4-DS* IgG4-related dacryoadenitis and sialadenitis, *MRI* magnetic resonance imaging, *SS* Sjögren's syndrome

dot-like calcifications on CT [20]; and small multiple cystic areas, which show hyperintensity on T2-weighted images.

### Statistical analysis

We calculated the sensitivity, specificity and accuracy using the following equations: sensitivity for IgG4-DS = a/(a+d+g), sensitivity for SS = e/(b+e+h), specificity = i/(c+f+i), accuracy = (a+e+i)/(a+b+c+d+e+f+g+h+i), where a: number of patients we diagnosed with IgG4-DS and who actually had IgG4-DS, b: number of patients we diagnosed with IgG4-DS but who had SS, c: number of patients we diagnosed with IgG4-DS but who were normal, d: number of patients we diagnosed with SS but who had IgG4-DS, e: number of patients we diagnosed with SS and who actually had SS, f: number of patients we diagnosed with SS but who were normal, g: number of patients we diagnosed as normal but who had IgG4-DS, h: number of patients we diagnosed as normal but who had SS, and i: number of patients we diagnosed as normal and who were actually normal. We performed the Bartlett test for the analysis of equal variance. To determine whether or not there were significant differences between two given groups among three, we performed the Steel-Dwass test in case of unequal variance, and the Tukey-Kramer test in case of equal variance using the statistical software JMP Pro 11.0 (SAS Institute, Cary, NC, USA). $p$ values <0.05 were considered significant. Intra-observer agreement rates between the repeat diagnoses (diagnosis carried out under blinded conditions and repeated after 3 weeks) were assessed with kappa values using 3 grades: 1 or 2, 3, and 4 or 5. Values <0.20 indicated poor agreement, 0.21–0.40 fair agreement, 0.41–0.60 moderate agreement, 0.61–0.80 good agreement and 0.81–1.00 excellent agreement.

## Results

Intra-observer agreement rates between the repeat diagnoses were very high. Kappa values for selecting the same diagnosis from normal, IgG4-DS or SS were 0.83 (range, 0.76–0.91) on sonography, 0.69 (range, 0.5–0.90) on FDG-PET/CT, 0.70 (range, 0.49–0.80) on CT and 0.80 (range, 0.64–0.87) on MRI. Moreover, average kappa values for each finding were 0.62 for sonography, 0.61 for FDG-PET/CT, 0.51 for CT and 0.54 for MRI; no findings showed an inverted order of scores the second time. Therefore, we have shown the results of the first diagnosis in the relevant figures.

### Analysis of sonographic findings

Figure 3 shows the results of sonographic analysis. In all findings, significant differences ($p \leq 0.0093$) were observed between any two of the three diagnoses. The parotid glands of patients with SS mainly exhibited multiple hypoechoic areas (median score 4) and hyperechoic lines and/or spots (median score 4) (Fig. 3a and b), while the reticular pattern in the parotid glands showed overlap between IgG4-DS (median score 1) and SS (median score 2) (Fig. 3c). In the submandibular glands, overlaps were seen between IgG4-DS and SS regarding the findings of multiple hypoechoic areas (median score 4 for both IgG4-DS and SS) and hyperechoic lines and/or spots (median score 3 for IgG4-DS and 4 for SS), although significant differences ($p = 0.0093$, $p < 0.0001$, respectively) were seen between the two (Fig. 3d and e). Obscuration of the submandibular gland configuration was mainly observed in SS (median score 3) (Fig. 3f). In contrast, IgG4-DS mainly exhibited reticular and nodal patterns (median score 5), and separation between IgG4-DS and the other conditions was especially good concerning the nodal pattern (median score 1 for normal glands and 2 for SS) (Fig. 3g and h). Intra-observer agreement rates between the repeat diagnoses were very high (kappa values, 0.67–0.87), which showed the nodal pattern could be easily detected.

Each case was diagnosed as normal, IgG4-DS or SS based on all of the sonographic findings. Sonographic

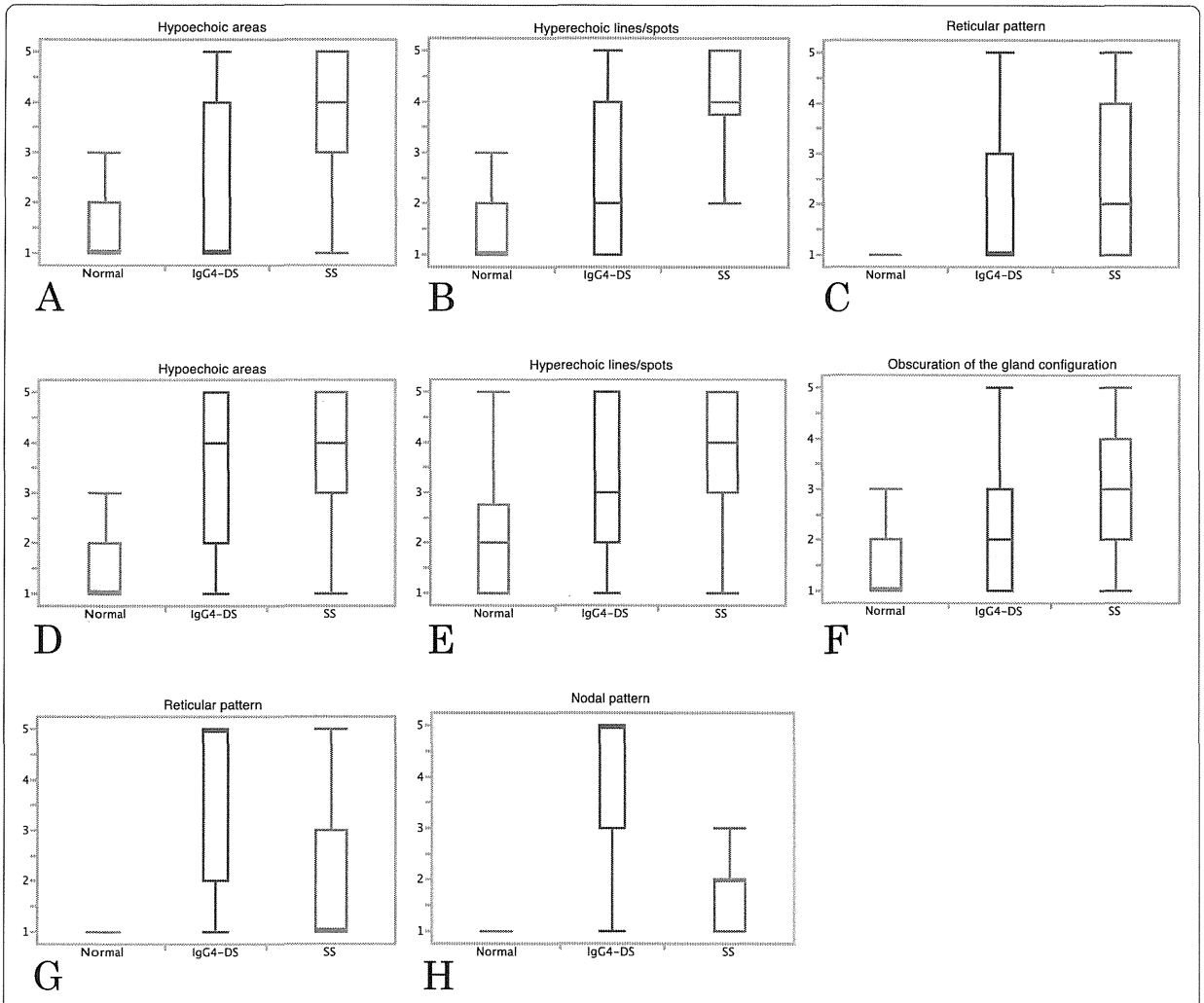


**Fig. 3** Results of sonographic analysis. Values are shown with median and quartile points for **a-c** the parotid glands and **d-h** the submandibular glands. **a** Multiple hypoechoic areas, **b** hyperechoic lines and/or spots and **c** reticular pattern in the parotid glands. **d** Multiple hypoechoic areas, **e** hyperechoic lines and/or spots, **f** obscuration of the gland configuration, **g** reticular pattern and **h** nodal pattern in the submandibular glands. Multiple hypoechoic areas (**a**) and hyperechoic lines and/or spots (**b**) in the parotid glands and obscuration of submandibular gland configuration (**f**) were primarily observed in patients with SS. Reticular and nodal patterns observed mainly in patients with IgG4-DS (**g, h**). *IgG4-DS* IgG4-related dacryoadenitis and sialadenitis, *SS* Sjögren's syndrome

sensitivity for detection of IgG4-DS and of SS, specificity and accuracy were 0.85, 0.80, 0.84 and 0.83, respectively.

### Analysis of FDG-PET/CT findings

FDG-PET/CT involving patients with IgG4-DS showed a tendency for abnormal accumulation of $^{18}$F-FDG and swelling of both the parotid (median scores 2 and 4, respectively) and submandibular glands (median scores 5 and 4, respectively) (Fig. 4a–d). Separation between IgG4-DS and the other conditions was particularly good regarding the abnormal accumulation of $^{18}$F-FDG in the submandibular glands (median score 2 for normal glands and 1 for SS) (Fig. 4c). In relation to this finding, significant differences were observed between IgG4-DS and SS ($p$ <0.0001), and between patients with IgG4-DS and those with normal glands ($p$ <0.0001); however, this was not seen between patients with normal glands and SS ($p$ = 0.1180). Intra-observer agreement rates between the repeat diagnoses were high (kappa values, 0.51–0.89). Regarding all other findings, significant differences ($p$ ≤0.0049) were observed between any two of three diagnoses.

Each case was diagnosed as normal, IgG4-DS or SS based on all of the findings from FDG-PET/CT. The sensitivity for detection of IgG4-DS and of SS, specificity and accuracy using FDG-PET/CT were 0.79, 0.59, 0.81 and 0.73, respectively.

### Analysis of CT findings

Figure 5 shows the results of CT findings concerning the parotid glands (Fig. 5a–c), and the submandibular glands (Fig. 5d and e). Patients with IgG4-DS had large parotid (median score 4) and submandibular glands (median score 4) (Fig. 5a and d). Although there were significant differences between normal glands (parotid glands, median score 3, $p$ = 0.0255; submandibular glands, median score 3, $p$ <0.0001), there seemed to be a similar tendency between these two. Conversely, patients with SS had small parotid (median score 3) and submandibular glands (median score 2), especially submandibular glands. Patients with SS had a high score regarding the finding of a salt-and-pepper appearance and/or dot-like calcification (median score 4) (Fig. 5b). Regarding this finding, significant differences were observed between the other two

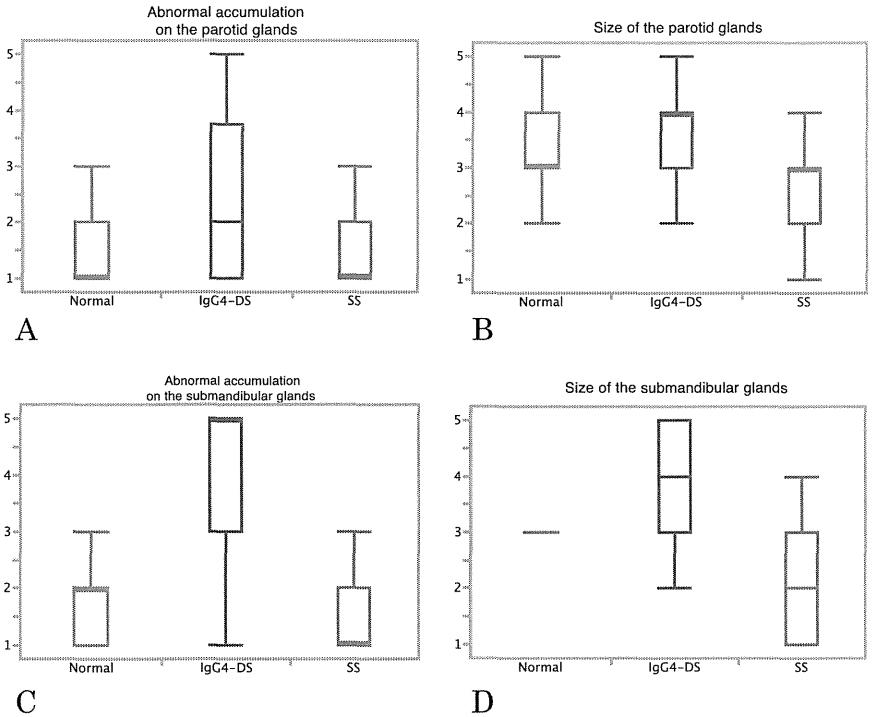


**Fig. 4** Results of FDG-PET/CT. Values are shown with median and quartile points for **a, b** the parotid glands and **c, d** the submandibular glands. **a** Abnormal accumulation of $^{18}$F-FDG in the parotid glands, **b** size of the parotid glands, **c** abnormal accumulation of $^{18}$F-FDG in the submandibular glands and **d** size of the submandibular glands. Abnormal accumulation of $^{18}$F-FDG and swelling of the glands in both the parotid and submandibular glands of a patient with IgG4-DS (**a-d**). Separation of IgG4-DS from the other conditions is especially good regarding the abnormal accumulation of $^{18}$F-FDG in the submandibular glands (**c**), and significant differences can be observed between IgG4-DS and SS ($p$ <0.0001), and between IgG4-DS and normal glands ($p$ <0.0001). *FDG-PET/CT* 2-[$^{18}$F]-fluoro-2-deoxy-D-glucose positron emission tomography/computed tomography, *IgG4-DS* IgG4-related dacryoadenitis and sialadenitis, *SS* Sjögren's syndrome

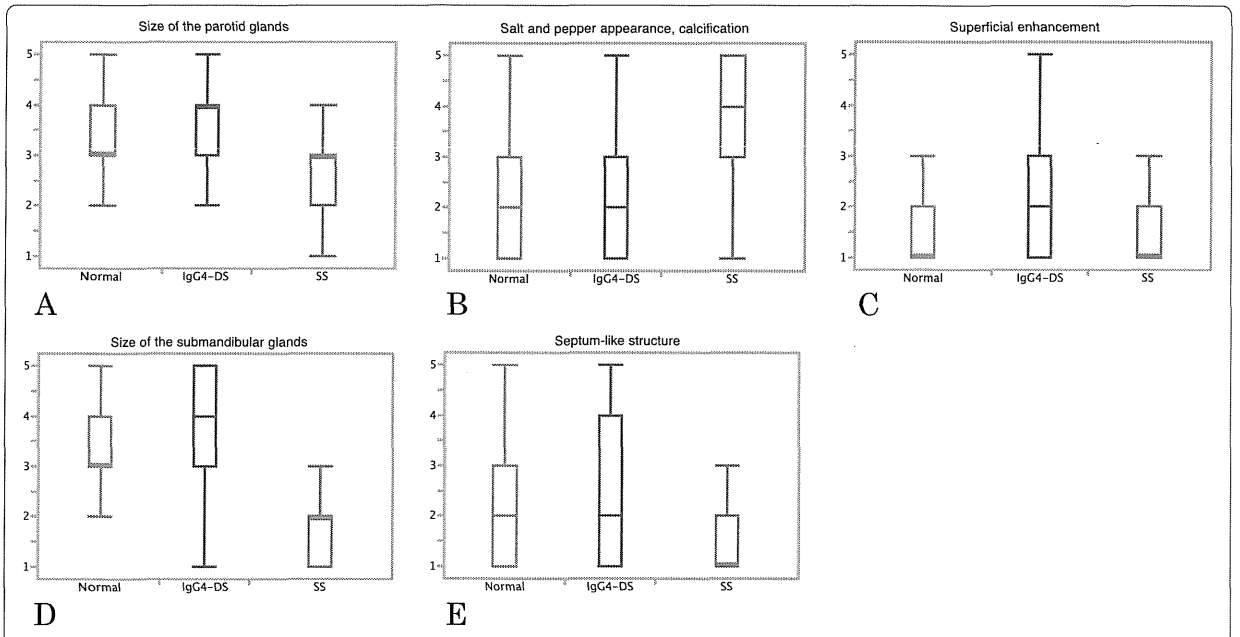


**Fig. 5** Results of CT. Values are shown with median and quartile points for **a-c** the parotid glands and **d, e** the submandibular glands. **a** Size of the parotid glands, **b** salt-and-pepper appearance and/or dot-like calcification in the parotid glands, **c** superficial enhancement of the parotid glands, **d** size of the submandibular glands and **e** septum-like structure in the submandibular glands. Patient with IgG4-DS exhibiting large parotid and submandibular glands (**a, d**). SS shows a high score in the finding of a salt-and-pepper appearance and/or dot-like calcification (**b**). *CT* computed tomography, *IgG4-DS* IgG4-related dacryoadenitis and sialadenitis, *SS* Sjögren's syndrome

conditions (median score 2 for both normal glands and IgG4-DS) ($p$ <0.0001), although this was not the case for between patients with normal glands and IgG4-DS ($p$ = 0.7945). Superficial enhancement of the parotid glands (median score 2 for IgG4-DS) (Fig. 5c) and the presence of a septum-like structure in the submandibular glands (median score 2 for IgG4-DS) (Fig. 5e), which we considered were some of the characteristic findings of IgG4-DS, showed significant differences between the other two conditions ($p$ <=0.0316); however, overlap was also observed and separation was not so good.

Each case was diagnosed as normal, IgG4-DS or SS based on all of the findings from CT. The sensitivity for detection of IgG4-DS and of SS, specificity and accuracy by CT were 0.64, 0.73, 0.70 and 0.70, respectively.

### Analysis of MRI findings

Figure 6 shows the results of MRI evaluation of the parotid glands (Fig. 6a–c), and the submandibular glands (Fig. 6d). Patients with IgG4-DS had large parotid (median score 4) and submandibular glands (median score 5) (Fig. 6a and d). These findings differed significantly between the other two conditions for both the parotid and submandibular glands ($p$ <0.0001). Conversely, patients with SS had small parotid (median score 3) and submandibular glands (median score 2), especially submandibular glands; there was a very clear separation between the other two conditions. Patients with SS had a high score regarding the finding of a salt-and-pepper appearance and/or multiple cystic areas in the parotid glands (median score 4.5) (Fig. 6b); there was also a very clear separation between the other two conditions (median score 1.5 for normal glands and 2 for IgG4-DS). Intra-observer agreement rates between the repeat diagnoses were high (kappa values, 0.54–0.79) regarding this finding. In relation to this finding, significant differences were observed between the other two conditions ($p$ <0.0001), although a significant difference was not seen between patients with normal glands and IgG4-DS ($p$ = 0.4163). Fatty degeneration in the parotid glands, which we considered to be one of the characteristic findings of SS, showed significant differences between the other two conditions ($p$ <=0.0061); however, overlap was also observed and separation was not so good.

Each case was diagnosed as normal, IgG4-DS or SS based on all of the findings. The sensitivity for detection of IgG4-DS and of SS, specificity and accuracy using MRI were 0.80, 0.67, 0.81 and 0.76, respectively.

### Comparison of the four imaging modalities

Figure 7 shows the sensitivity, specificity and accuracy of the four imaging modalities; sonography showed the highest levels. Regarding the sensitivity of IgG4-DS, there were significant differences between CT and the

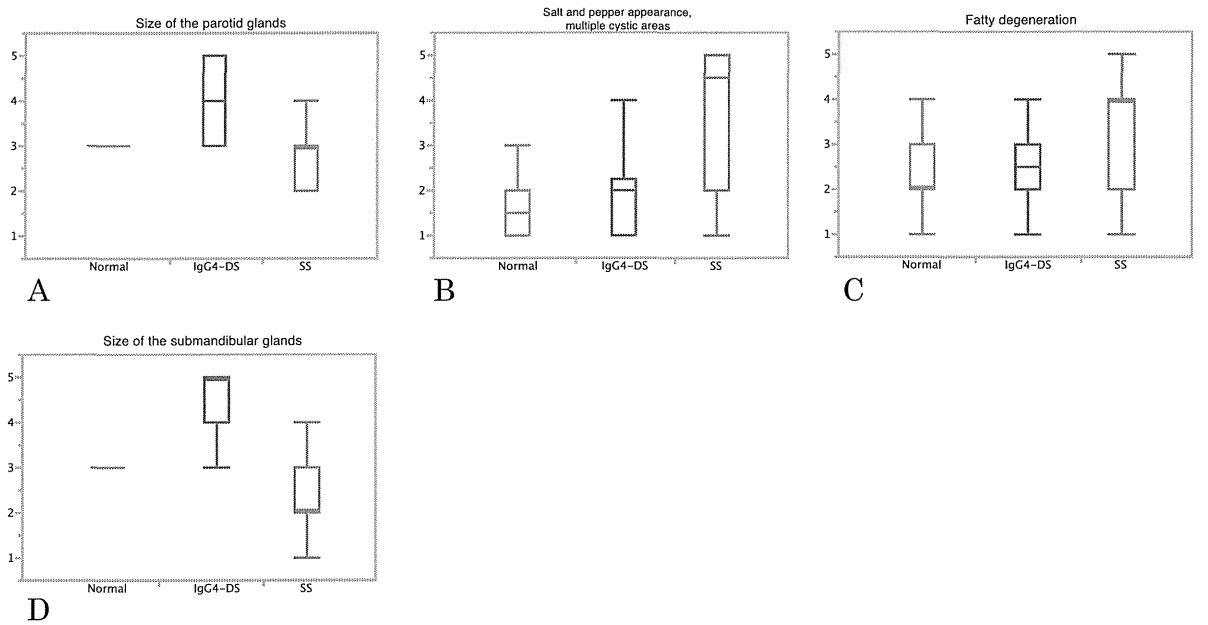


**Fig. 6** Results of MRI. Values are shown with median and quartile points for (**a-c**) the parotid glands and (**d**) the submandibular glands. **a** Size of the parotid glands, **b** salt-and-pepper appearance and/or multiple cystic areas in the parotid glands, **c** fatty degeneration of the parotid glands and **d** size of the submandibular glands. Patient with IgG4-DS showing large parotid and submandibular glands (**a, d**). SS shows small parotid and submandibular glands (**a, d**), and a high score in the finding of a salt-and-pepper appearance and/or multiple cystic areas in the parotid glands (**b**). *IgG4-DS* IgG4-related dacryoadenitis and sialadenitis, *MRI* magnetic resonance imaging, *SS* Sjögren's syndrome

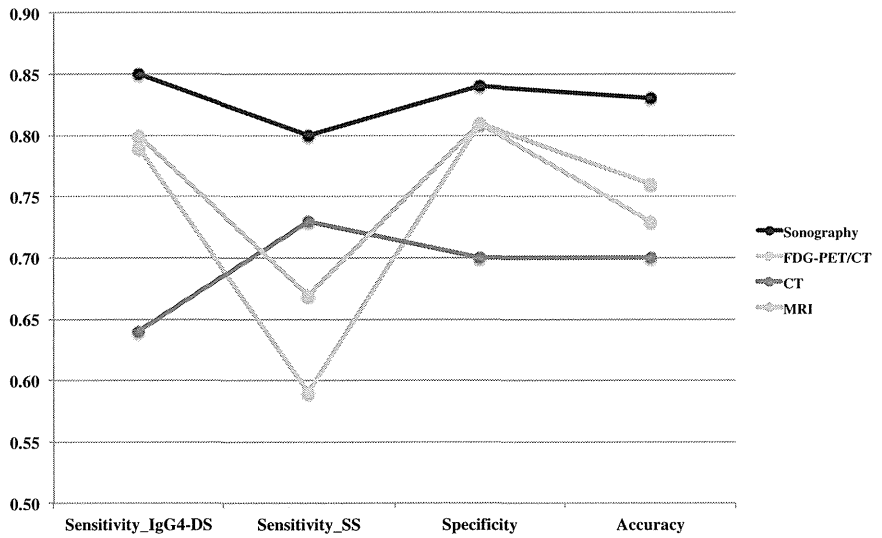


**Fig. 7** Sensitivity, specificity and accuracy of the four imaging modalities. Values are the average for all observers of each modality. Sonography showed not only the highest accuracy, but also the highest sensitivity for both IgG4-DS and SS, and the highest specificity among the modalities. There were significant differences between sonography and CT ($p = 0.0001$) and between sonography and FDG-PET/CT ($p = 0.0058$) regarding accuracy. *CT* computed tomography, *FDG-PET/CT* 2-[$^{18}$F]-fluoro-2-deoxy-D-glucose positron emission tomography/computed tomography, *IgG4-DS* IgG4-related dacryoadenitis and sialadenitis, *MRI* magnetic resonance imaging, *SS* Sjögren's syndrome

other three modalities ($p$ <0.001). Concerning the sensitivity of SS, there were significant differences between sonography and FDG-PET/CT ($p$ = 0.0004) and between CT and FDG-PET/CT ($p$ = 0.0180). In relation to specificity, there were significant differences between sonography and CT ($p$ = 0.0463). Regarding the accuracy, there were significant differences between sonography and CT ($p$ = 0.0001) and between sonography and FDG-PET/CT ($p$ = 0.0058); however, there were no significant differences between sonography and MRI ($p$ = 0.0796).

## Discussion

For screening IgG4-DS, the nodal pattern of the submandibular glands on sonograms and the abnormal accumulation of $^{18}$F-FDG in the submandibular glands on FDG-PET/CT were very effective. However, the effective findings regarding the screening of SS were a salt-and-pepper appearance and/or multiple cystic areas in the parotid glands on MRI. Taking into consideration high sensitivity for both IgG4-DS and SS, and high specificity in addition to high accuracy, the most effective imaging modality was sonography.

We did not include images of the lacrimal glands. Even if they were included, we could detect the affected lacrimal glands as a nodal pattern on sonograms, as abnormal $^{18}$F-FDG accumulation on FDG-PET/CT, and as abnormal swelling on CT and MRI. Consequently, the abnormal findings of images of the lacrimal glands would raise the accuracy of all modalities equally, and the effectiveness of each modality would not change appreciably.

### Sonography

Sonography provided useful information regarding the screening of IgG4-DS. The nodal and reticular patterns, often with normal parenchyma surrounding the affected region and located bilaterally, were easily detected in the submandibular glands even by inexperienced observers. When the sublingual glands are affected, they also show a nodal and/or reticular pattern on sonograms (data not shown); therefore, it would be easier to make an accurate diagnosis. Using sonography, not only IgG4-DS but also SS can be detected. Multiple hypoechoic areas and hyperechoic lines and/or spots in the parotid glands achieved high scores. These findings might be misleading, because IgG4-DS sometimes exhibits similar findings. However, hypoechoic areas of IgG4-DS were observed in the normal parotid parenchyma without a reduction in the echo intensity level and heterogeneity. Moreover, IgG4-DS mainly affects the submandibular glands, and most of the cases present with normal parotid glands [9]. Conversely, SS shows atrophic changes in both the parotid and submandibular glands. Therefore, the combination of parotid and submandibular gland findings could lead to accurate diagnosis. In the present study we only analyzed B-mode sonograms. If Doppler images are added, it can make differentiation between IgG4-DS and SS much easier. The nodal and reticular patterns of IgG4-DS show high vascularity [9], while SS exhibits small dot-like vascularity in the parotid glands [22]. When the IgG4-DS patients had shown submandibular gland swelling and salivary gland tumors had been suspected, sonography revealed nodal and/or reticular changes on both sides, and tumorous lesions were easily ruled out.

### FDG-PET/CT

FDG-PET/CT showed abnormal $^{18}$F-FDG accumulation in the glands affected with IgG4-DS. However, this imaging modality could not differentiate between normal glands and SS. Patients with SS do not undergo FDG-PET/CT, unless they have other malignant diseases. Our cases involving FDG-PET/CT were patients with SS who were partly suspected of having malignant lymphoma. When patients actually had lymphoma, the SUV was high and we could not differentiate the disease from IgG4-DS. Conversely, very severe SS with atrophic submandibular glands exhibited a very low SUV both in the parotid and submandibular glands. In contrast, SS patients in the lower stages (their sialography showed punctuate or globular patterns) had a rather high SUV (SUV; 3–4). This finding was in accordance with a report by Cohen et al. [23]. Normal salivary, sublingual, submandibular and parotid glands sometimes show high SUVs. Because Nakamoto et al. have reported that the intensity of $^{18}$F-FDG uptake in the salivary glands is variable [24], we need to carefully differentiate IgG4-DS from normal variances.

### CT and MRI

Nodal changes in IgG4-DS detected using sonography were not clearly observed on CT or MRI. In some cases CT and MRI displayed superficial enhancement in the parotid glands of IgG4-DS. However, unspecific swelling of the parotid and submandibular glands was observed in general. Most of the patients with normal salivary glands, that were large in size, were misdiagnosed as IgG4-DS. Some of our cases showed slightly low signal intensity on T2-weighted images on MRI; however, they were not significant. These results were not in accordance with the very low signal intensity on T2-weighted images [12, 13]. This may be because of the limited number of our MRI of the IgG4-DS patients. Diffusion-weighted images might differentiate nodal changes regarding IgG4-DS more clearly. SS, however, showed a characteristic salt-and-pepper appearance on CT and MRI. When this appearance was not pronounced, inexperienced observers could not detect it on CT.

Two things are important in diagnosing IgG4-DS. The first is to differentiate malignant lymphoma. Malignant lymphoma sometimes affects salivary glands, and can appear in bilateral glands, which mimic IgG4-DS [25]. To make a final diagnosis, biopsy is recommended. Second, IgG4-DS does not always occur simultaneously in both the lacrimal and salivary glands. Even if the findings are indefinite at the time of examination, follow-up is necessary when IgG4-DS is suspected.

## Conclusions

Changes in the submandibular glands affected by IgG4-DS, which often occur bilaterally, could be easily detected using sonography as a result of characteristic bilateral nodal/reticular changes and by FDG-PET/CT because of abnormal $^{18}$F-FDG accumulation. Even inexperienced observers could detect these findings. In addition to IgG4-DS, sonography could also differentiate SS. Therefore, we recommend sonography as a modality for the screening of IgG4-DS, because it is easy to use, does not involve radiation exposure and is an effective imaging modality.

### Abbreviations

AIP: autoimmune pancreatitis; CT: computed tomography; FDG-PET/CT: 2-[$^{18}$F]-fluoro-2-deoxy-D-glucose positron emission tomography/computed tomography; IgG4: immunoglobulin G4; IgG4-DS: IgG4-related dacryoadenitis and sialadenitis; IgG4-RD: IgG4-related disease; MHz: megahertz; MRI: magnetic resonance imaging; SS: Sjögren's syndrome; SUV: standardized uptake value.

### Competing interests

The authors declare that they have no competing interests.

### Authors' contributions

MS was responsible for study design, literature review, imaging data collection, data analysis, manuscript writing and editing. KO, YK, YT, HF and WW participated in imaging data collection, data interpretation, data analysis and critical revision of the manuscript. MM, YO and SF were responsible for clinical data collection and critical revision of the manuscript. SN and KY were responsible for study design, supervised the study and critical revision of the manuscript. All the authors read and approved the final manuscript.

### Acknowledgements

This study was supported in part by grants from the Ministry of Education, Culture, Sports, Science and Technology of Japan (24592835).

### Author details

[1]Department of Oral and Maxillofacial Radiology, Kyushu University Hospital, 3-1-1 Maidashi, Higashi-ku, Fukuoka 812-8582, Japan. [2]Department of Oral and Maxillofacial Radiology, Faculty of Dental Science, Kyushu University, 3-1-1 Maidashi, Higashi-ku, Fukuoka 812-8582, Japan. [3]Department of Oral and Maxillofacial Radiology, School of Dentistry, Aichi Gakuin University, 1-100 Kusumoto-cho, Chikusa-ku, Nagoya 464-8650, Japan. [4]Section of Oral and Maxillofacial Oncology, Division of Maxillofacial Diagnostic and Surgical Sciences, Kyushu University, 3-1-1 Maidashi, Higashi-ku, Fukuoka 812-8582, Japan. [5]Section of Oral and Maxillofacial Surgery, Division of Maxillofacial Diagnostic and Surgical Sciences, Kyushu University, 3-1-1 Maidashi, Higashi-ku, Fukuoka 812-8582, Japan.

Received: 15 April 2015 Accepted: 10 August 2015
Published online: 23 August 2015

### References

1. Tsubota K, Fujita H, Tsuzaka K, Takeuchi T. Mikulicz's disease and Sjögren's syndrome. Invest Ophthalmol Vis Sci. 2000;41:1666–73.
2. Yamamoto M, Harada S, Ohara M, Suzuki C, Naishiro Y, Yamamoto H, et al. Clinical and pathological differences between Mikulicz's disease and Sjögren's syndrome. Rheumatology. 2005;44:227–34.
3. Yamamoto M, Takahashi H, Sugai S, Imai K. Clinical and pathological characteristics of Mikulicz's disease (IgG4-related plasmacytic exocrinopathy). Autoimmunity Rev. 2005;4:195–200.
4. Wallace ZS, Deshpande V, Mattoo H, Mahajan VS, Kulikova M, Pillai S, et al. IgG4-related disease: clinical and laboratory features in 125 patients. Arthritis Rheumatol. 2015; doi: 10.1002/art.39205. Epub 2015 May 18.
5. Ishii S, Shishido F, Miyajima M, Sakuma K, Shigihara T, Kikuchi K. Whole-body gallium-67 scintigraphic findings in IgG4-related disease. Clin Nucl Med. 2011;36:542–5.
6. Ishii S, Miyajima M, Sakuma K, Kikuchi K, Shishido F. Comparison between sarcoidosis and IgG4-related disease by whole-body 67Ga scintigraphy. Nucl Med Commun. 2013;34:13–8.
7. Ebbo M, Grados A, Guedj E, Gobert D, Colavolpe C, Zaidan M, et al. Usefulness of 2-[18F]-fluoro-2-deoxy-d-glucose-positron emission tomography/computed tomography for staging and evaluation of treatment response in IgG4-related disease: a retrospective multicenter study. Arthritis Care Res (Hoboken). 2014;66:86–96.
8. Zhang J, Chen H, Ma Y, Xiao Y, Niu N, Lin W, et al. Characterizing IgG4-related disease with 18F-FDG PET/CT: a prospective cohort study. Eur J Nucl Med Mol Imaging. 2014;41:1624–34.
9. Shimizu M, Moriyama M, Okamura K, Kawazu T, Chikui T, Goto TK, et al. Sonographic diagnosis for Mikulicz disease. Oral Surg Oral Med Oral Pathol Oral Radiol Endod. 2009;108:105–13.
10. Asai S, Okami K, Nakamura N, Shiraishi S, Sugimoto R, Anar D, et al. Localized or diffuse lesions of the submandibular glands in immunoglobulin g4-related disease in association with differential organ involvement. J Ultrasound Med. 2013;32:731–6.
11. Takagi Y, Nakamura H, Origuchi T, Miyashita T, Kawakami A, Sumi M, et al. IgG4-related Mikulicz's disease: ultrasonography of the salivary and lacrimal glands for monitoring the efficacy of corticosteroid therapy. Clin Exp Rheumatol. 2013;31:773–5.
12. Katsura M, Mori H, Kunimatsu A, Sasaki H, Abe O, Machida T, et al. Radiological features of IgG4-related disease in the head, neck, and brain. Neuroradiology. 2012;54:873–82.
13. Fujita A, Sakai O, Chapman MN, Sugimoto H. IgG4-related disease of the head and neck: CT and MR imaging manifestations. Radiographics. 2012;32:1945–58.
14. Okazaki K, Kawa S, Kamisawa T, Shimosegawa T, Tanaka M. Research Committee for Intractable Pancreatic Disease and Japan Pancreas Society. Japanese consensus guidelines for management of autoimmune pancreatitis: I. Concept and diagnosis of autoimmune pancreatitis. J Gastroenterol. 2010;45:249–65.
15. Yamamoto M, Takahashi H, Ohara M, Suzuki C, Naishiro Y, Yamamoto H, et al. A new conceptualization for Mikulicz's disease as an IgG4-related plasmacytic disease. Mod Rheumatol. 2006;16:335–40.
16. Fujibayashi T, Sugai S, Miyasaka N, Hayashi Y, Tsubota K. Revised Japanese criteria for Sjögren's syndrome (1999): availability and validity. Mod Rheumatol. 2004;14:425–34.
17. Vitali C, Bombardieri S, Jonsson R, Moutsopoulos HM, Alexander EL, Carsons SE, et al. Classification criteria for Sjogren's syndrome: a revised version of the European criteria proposed by the American–European Consensus Group. Ann Rheum Dis. 2002;61:554–8.
18. Takagi Y, Kimura Y, Nakamura H, Sasaki M, Eguchi K, Nakamura T. Salivary gland ultrasonography: can it be an alternative to sialography as an imaging modality for Sjogren's syndrome? Ann Rheum Dis. 2010;69:1321–4.
19. Shimizu M, Okamura K, Yoshiura K, Ohyama Y, Nakamura S, Kinukawa N. Sonographic diagnostic criteria for screening Sjögren's syndrome. Oral Surg Oral Med Oral Pathol Oral Radiol Endod. 2006;102:85–93.
20. Sun Z, Zhang Z, Fu K, Zhao Y, Liu D, Ma X. Diagnostic accuracy of parotid CT for identifying Sjögren's syndrome. Eur J Radiol. 2012;81:2702–9.
21. Takashima S, Takeuchi N, Morimoto S, Tomiyama N, Ikezoe J, Shogen K, et al. MR imaging of Sjögren syndrome: correlation with sialography and pathology. J Comput Assist Tomogr. 1991;15:393–400.
22. Shimizu M, Okamura K, Yoshiura K, Ohyama Y, Nakamura S. Sonographic diagnosis of Sjögren syndrome: evaluation of parotid gland vascularity as a diagnostic tool. Oral Surg Oral Med Oral Pathol Oral Radiol Endod. 2008;106:587–94.
23. Cohen C, Mekinian A, Uzunhan Y, Fauchais AL, Dhote R, Pop G, et al. 18F-fluorodeoxyglucose positron emission tomography/computer tomography

as an objective tool for assessing disease activity in Sjögren's syndrome. Autoimmun Rev. 2013;12:1109–14.
24. Nakamoto Y, Tatsumi M, Hammoud D, Cohade C, Osman MM, Wahl RL. Normal FDG distribution patterns in the head and neck: PET/CT evaluation. Radiology. 2005;234:879–85.
25. Ohta M, Moriyama M, Goto Y, Kawano S, Tanaka A, Maehara T, et al. A case of marginal zone B cell lymphoma mimicking IgG4-related dacryoadenitis and sialoadenitis. World J Surg Oncol. 2015;13:459. doi:10.1186/s12957-015-0459-z. Epub 2015 Feb 21.

Japan College of Rheumatology
MODERN RHEUMATOLOGY

http://informahealthcare.com/mor
ISSN 1439-7595 (print), 1439-7609 (online)

Mod Rheumatol, 2014; Early Online: 1–6

DOI: 10.3109/14397595.2014.990674

informa
healthcare

ORIGINAL ARTICLE

# Total lesion glycolysis as an IgG4-related disease activity marker

Yoshinari Nakatsuka[1], Tomohiro Handa[1], Yuji Nakamoto[2], Tomomi Nobashi[2], Hajime Yoshihuji[3], Kiminobu Tanizawa[4], Kohei Ikezoe[1], Akihiko Sokai[1], Takeshi Kubo[2], Toyohiro Hirai[1], Kazuo Chin[4], Kaori Togashi[2], Tsuneyo Mimori[3], and Michiaki Mishima[1]

[1]*Department of Respiratory Medicine, Graduate School of Medicine, Kyoto University, Kyoto, Japan,* [2]*Department of Diagnostic Imaging and Nuclear Medicine, Graduate School of Medicine, Kyoto University, Kyoto, Japan,* [3]*Department of Rheumatology and Clinical Immunology, Graduate School of Medicine, Kyoto University, Kyoto, Japan, and* [4]*Department of Respiratory Care and Sleep Control Medicine, Graduate School of Medicine, Kyoto University, Japan*

**Abstract**

*Objectives.* 2-[18F]-fluoro-2-deoxy-D-glucose-positron emission tomography/computed tomography (FDG-PET/CT) was reported to be useful for monitoring immunoglobulin G4-related disease (IgG4-RD); however, a quantitative FDG-PET/CT analysis such as total lesion glycolysis (TLG) has not yet been conducted. This study aimed to investigate whether TLG would correlate with serum markers in IgG4-RD, and the utility of TLG for disease monitoring.

*Methods.* This retrospective study included 17 patients (12 men; median age, 62 years) who were followed up at Kyoto University Hospital and underwent FDG-PET/CT from April 2009 to November 2013. TLG was calculated for the involved lesions. Correlations between serum markers [IgG4, soluble IL-2 receptor (sIL-2R), lactate dehydrogenase (LDH), and C-reactive protein (CRP)] and TLG concomitant with FDG-PET/CT scans were investigated. Serial changes in TLG were assessed in patients who underwent follow-up FDG-PET/CT ($n = 6$).

*Results.* The calculated median (IQL) TLG value was 154.8 (63.7–324.4). A significant correlation was found between the sIL-2R level and TLG ($P = 0.001$, rs = 0.763). In contrast, no correlations were found between the IgG4, LDH, or CRP levels and TLG. Increased or decreased TLG corresponded with clinical disease improvement or worsening.

*Conclusions.* TLG correlated significantly with the serum sIL-2R level and may be useful for disease monitoring in IgG4-RD.

**Keywords**

FDG-PET, IgG4-related disease, Soluble IL-2 receptor, Total lesion glycolysis

**History**

Received 7 August 2014
Accepted 19 November 2014
Published online 29 December 2014

## Introduction

Immunoglobulin G4-related disease (IgG4-RD) is a multiorgan disease that is histologically characterized by the marked infiltration of IgG4-positive plasma cells into affected organs and elevated serum IgG4 levels [1,2]. Commonly affected sites include the pancreas (autoimmune pancreatitis), salivary glands (Mikulicz disease), retroperitoneal space (retroperitoneal fibrosis), lymph nodes, and lungs [3]. To date, there are no established clinical indices for evaluating IgG4-RD activity [4].

2-[18F]-fluoro-2-deoxy-D-glucose-positron emission tomography/computed tomography (FDG-PET/CT) is a commonly used diagnostic tool for malignant diseases. FDG-PET/CT has been reported to be useful for lesion detection and disease activity evaluations in IgG4-RD cases [4,5]. A major advantage of FDG-PET/CT is that it provides quantitative data regarding lesion metabolic activity on a whole-body scale [5]. Total lesion glycolysis (TLG) is a recently proposed FDG uptake parameter; this parameter is calculated as the mean standardized uptake value (SUVmean) × the metabolic tumor volume (MTV). TLG reflects the total FDG uptake in the lesion, and a summation of TLG value from each lesion can indicate global metabolic disease activity in patients with multiorgan disorder [6]. However, there is no paper that investigated TLG in IgG4-RD; therefore, it is unknown in IgG4-RD patients whether TLG correlates serum markers of inflammations and whether serial change of TLG coincides with clinical course.

In the present study, to evaluate the utility of TLG for assessing IgG4-RD activity, we calculated the TLG values of IgG4-RD patients and determined whether these values correlated with serum levels of inflammatory biomarkers. Additionally, we compared changes in TLG with clinical courses of patients who underwent serial FDG-PET/CT studies.

## Materials and methods

### Study subjects

This retrospective study included 17 patients (12 men and 5 women) who were diagnosed with definite IgG4-RD at Kyoto University Hospital and underwent FDG-PET/CT before the initiation of immunosuppressive therapy during the period from April 2009 to November 2013. Seven of these cases were recurrent for which corticosteroid or immunosuppressive therapy had not been administered within 6 months prior to the FDG-PET/CT scan. The diagnoses were based on the criteria proposed by Umehara et al. [1]. Only the definite cases were included which fulfilled all of the following criteria: characteristic lesion

Correspondence to: Tomohiro Handa, MD, PhD, Department of Respiratory Medicine Graduate School of Medicine, Kyoto University, 54 Shogoin Kawaharacho, Sakyo-ku, Kyoto 606-8507. Tel: + 81-75-751-3830. Fax: + 81-75-751-4643. E-mail: hanta@kuhp.kyoto-u.ac.jp

distribution, an elevated serum IgG4 level (> 135 mg/dL), and histopathological findings compatible with IgG4-RD. The median (interquartile) age at the first test was 62 (range, 58 – 73) years. Patients initially underwent FDG-PET/CT because of suspected malignant disease (e.g., malignant lymphoma) and were ultimately diagnosed with IgG4-RD. Patients were excluded from study if FDG-PET/CT had been performed at an institute other than Kyoto University Hospital, or if corticosteroid or another immunosuppressive therapy had been administered at the time of the initial FDG-PET/CT scan. Patients with active malignant diseases were excluded; however, three cases with histories of malignancies within 5 years prior to FDG-PET/CT (thyroid cancer, colon cancer, and double lung and breast cancer) were included because in each case, radical treatment had been performed and malignant recurrence had been clinically excluded.

Twelve patients were symptomatic, and salivary gland swelling and hydronephrosis-related symptoms such as abdominal pain were comparatively common, whereas five cases did not complain of any symptoms. Comorbidities included diabetes mellitus in three cases, bronchial asthma in two and Grave's disease in two; in all cases the comorbid diseases were well controlled. The number of involved organs varied with a maximum of eight affected organs. Thirteen patients received corticosteroid therapy at a median (interquartile) dose of 35 (31.3 – 36) mg/day upon conversion to prednisolone. Patient characteristics are summarized in Table 1.

The Kyoto University Hospital Institutional Review Board approved this study (E201).

### FDG-PET/CT imaging

PET/CT scan was performed on a combined PET/CT scanner (Discovery ST Elite; GE Healthcare, Little Chalfont, UK). Patients fasted for at least 4 h before the study and after the plasma glucose level was confirmed to be < 150 mg/dL, each patient received an intravenous administration of a standard dose of 3.7MBq/kg of FDG. Approximately 60 min after the injection, a low-dose CT scan and successive PET scan covering the levels from the upper thigh to the skull was performed while the patient maintained shallow breathing. In this PET/CT scan system, CT and PET images were coregistered and the CT data were used for attenuation correction. These images were reconstructed using the VUE Point Plus 3-dimensional iterative reconstruction algorithm.

Table 1. Patient characteristics.

| | All patients, N = 17 |
|---|---|
| Sex, male/female | 12/5 |
| Age, years | 66 (57–73) |
| Symptoms | |
| Symptomatic* | 12 |
| Hydronephrosis-related symptoms | 6 |
| Salivary gland swelling | 2 |
| Exophthalmos | 3 |
| Dry mouth or dry eye | 2 |
| Asymptomatic | 5 |
| Comorbidities | |
| Hypertension | 5 |
| Diabetes | 3 |
| Asthma | 2 |
| Grave's disease | 2 |
| Angina pectoris | 2 |
| Number of involved organs | |
| 1 | 4 |
| 2 | 4 |
| 3 | 3 |
| 4 | 4 |
| 5 ≦ | 2 |
| Serum IgG, mg/dl | 2179 (1820–2761) |
| Serum IgE, mg/dl | 740 (400–1100) |
| Corticosteroid therapy | 13 |
| Initial corticosteroid dose, mg/day | 35 (32.3–36) |

Values are presented as medians (interquartile ranges) or numbers.
*MTV* metabolic tumor volume, *TLG* total lesion glycolysis, *sIL-2R* soluble interleukin- 2 receptor, *IgG4* immunoglobulin G4.
*One patient complained of abdominal pain due to hydronephrosis as well as dry mouth and was counted separately.

### Image interpretation

All images were reviewed for consensus by two observers (one nuclear medicine physician and one pulmonary physician). FDG accumulation was assessed on a workstation (Advantage Workstation, GE Healthcare) by calculating the standardized uptake value (SUV) in the regions of interest. SUV was calculated using the following formula: SUV = Cdc/(Di/W), where Cdc is the decay-corrected tracer tissue concentration (in Bq/g); Di is the injected dose (in Bq); and W is the patient's body weight (in g). Abnormal FDG uptake was identified based on a visual comparison of FDG uptake between the background organ and target site. All sites with abnormal FDG uptake were considered approximate foci of IgG4-RD lesions, although pathological analysis was not available for all sites. Next, we manually drew a 3D cuboid contour surrounding the abnormal uptake site. Within this contour, the voxels with SUV equal to or greater than the cut-off value were automatically extracted and defined as the optimal lesion border (Figure 1). In the present study, the cut-off value was fixed at 2.5 in accordance with previous reports [7–10]. The lesion volume was calculated as the metabolic tumor volume (MTV). The average SUV in the lesion was defined as the SUVmean, and TLG was calculated as the product of SUVmean and MTV [6]. After calculating the TLG of all affected lesions, we summed the TLG of each lesion to generate a final TLG score for each patient.

Furthermore, as FDG is excreted into the urine, kidneys or urinary ducts show a physiologically high uptake of FDG; therefore, we considered that the physiological uptake of FDG in urine was inevitably included when evaluating kidney lesions. To account for this, two observers carefully excluded the urinary tract or a healthy area of kidney by the visual assessment based on a CT scan. Moreover, to minimize the influence of physiological urine uptake, we subtracted the FDG uptake of urine from that of each lesion. SUVmax of the lesions other than those of the kidney did not exceed 10.0 in the present study; therefore, we defined the areas with SUV > 10 as urine uptake. Finally, we calculated the TLG of

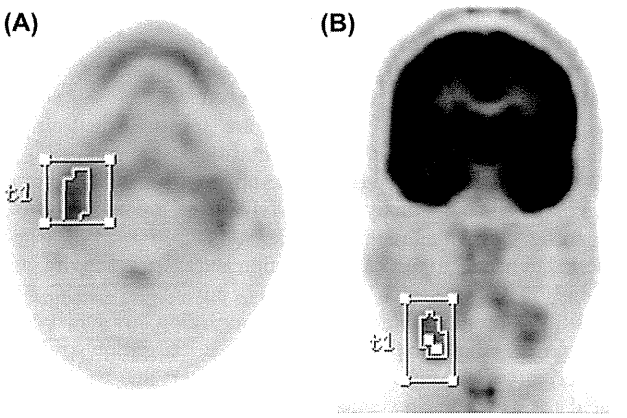


Figure 1. TLG measurement in a 47-year-old male with a salivary gland lesion. Sample coronal (A) and axial (B) PET images with quantitative parameters from a workstation are shown. Within the three-dimensional cuboid contour surrounding the right submandibular gland, voxels equal to or greater than the cut-off value (2.5) were automatically extracted. In this lesion, the maximum SUVmax, MTV, and TLG were 3.2, 6.5, and 18.1, respectively.

the area with an SUV > 10.0 within the contour and subtracted this from the TLG of the area with an SUV > 2.5. In addition, to completely exclude the influence of physiological urine excretion, we also performed sub-analysis in patients without renal lesions.

In this study, a maximum value of SUV within the region (SUVmax) of all affected organs was also assessed. When SUVmax was below 2.5, it was recorded as < 2.5. Owing to the methodological limitation, physiological excretion in the urine may influence SUVmax more strongly than TLG. Therefore, patients with kidney lesions were excluded when SUVmax was used in this analysis.

### Laboratory data

Laboratory data were obtained from the medical records. The serum C-reactive protein (CRP), lactate dehydrogenase (LDH), soluble IL-2 receptor (sIL-2R), and IgG4 concentrations were included if the evaluations had been conducted within 2 months before FDG-PET/CT. Laboratory evaluations after FDG-PET/CT were allowed for those who did not receive treatment. Next, correlations between initial TLG or SUVmax values and serum markers were investigated in all patients.

All serum CRP and LDH tests were performed within 1 month before or after FDG-PET/CT. For sIL-2R and IgG4, 13 and 11 tests were performed within 1 month before or after FDG-PET/CT, respectively. Three and two cases lacked sIL-2R and IgG4 data, respectively.

### Follow-up study

Among patients who underwent a follow-up FDG-PET/CT study, serial changes in TLG between initial and follow-up studies were evaluated and increasing or decreasing trends were assessed. Next, an assessment of each patient's course of global disease activity course was made from the 2 physicians' consensus. The course of disease activity was assessed based on image findings other than FDG-PET/CT, patients' symptoms, and physical finding [11]. The temporal change regarding each parameter was classified according to a three-grade system (improved, no change, or worsened), and the global disease course was determined by considering each temporal change. In brief, when classification of each parameter matched, the global disease course was judged according to that specific classification. When a conflicting case existed (such as a case when some parameters both improved and worsened), it was agreed that a decision would be made according to the most significant finding judged by each observer; however, no such case occurred within this study. We investigated whether the trend in serial TLG change and SUVmax change coincided with the global activity course.

### Statistical analysis

Statistical analyses were performed using modified R software programs (The R Foundation for Statistical Computing, Perugia, Italy) as described previously [12,13]. Continuous data were presented as medians with interquartile ranges (IQR). The Spearman rank correlation coefficient test was used to analyze correlations between TLG and serum markers. A P-value of $< 0.05$ was considered statistically significant.

## Results

### Organs with abnormal FDG uptake

Organs with abnormal FDG uptake are listed in Table 2. Most affected organs exhibited positive FDG uptake, while there was no area with an SUV > 2.5 in any normal organ except for the kidney and intraorbital space (likely due to the physiological uptake of urine or external ocular muscles, respectively). Among these organs, the hilar and mediastinal lymph nodes were the most commonly affected, followed by the salivary glands. In contrast, three suspected lesions did not show abnormal FDG uptake. Two of these were typical of IgG4-RD lung involvement (one was a ground-glass opacity with interlobular septum thickening and reticular shadow and the other was a peribronchovascular infiltrative shadow with ill-defined nodules), and the third was a space-occupying pancreatic lesion with a 5-mm diameter that was identified by abdominal echography. Pathological examinations were not conducted for these three lesions.

Table 2. Organs with abnormal FDG uptake.

| Organs with abnormal FDG uptake | n* |
|---|---|
| Lacrimal gland | 1 |
| Intraorbital space | 3 |
| Salivary gland | 9 |
| Pharyngolarynx | 1 |
| Supraclavicular lymph nodes | 3 |
| Hilar/mediastinal lymph nodes | 13 |
| Lung | 2 |
| Pancreas | 1 |
| Kidney | 3 |
| Thoracic aorta | 1 |
| Abdominal aorta | 1 |
| Retroperitoneal fibrosis | 5 |
| Prostate | 5 |

*We counted multiple lesions within in a single organ as an one-organ lesion.

### Quantitative analysis of FDG-PET/CT and serum markers

Quantitative analyses of the FDG-PET/CT and serum biomarker data are summarized in Table 3. The median MTV was 51.4 mL (20.2–92.5 mL) and TLG was 154.8 (63.7–324.4). The serum CRP (median: 0.2 mg/dL, IQR: 0.1–0.5 mg/dL) and LDH (median: 170 IU/L, IQR: 157–192 IU/L) levels were normal or slightly elevated in a majority of the cases. In contrast, elevated sIL2-R (median: 871.5 U/mL, IQR: 652.5 − 1337.5 U/mL) and IgG4 (median: 736 mg/dL, IQR: 539–1150 mg/dL) levels were observed.

### Correlations between TLG and serum markers

Among the serum markers investigated in the present study, sIL-2R levels were found to significantly, positively correlate with TLG ($P = 0.001$, rs = 0.763) and SUVmax ($P = 0.018$, rs = 0.723). CRP ($P = 0.913$, rs = 0.029), LDH ($P = 0.444$, rs = − 0.199), and IgG4 ($P = 0.192$, rs = 0.357) levels did not significantly correlate with either TLG or SUVmax (Figure 2, Supplementary Figure 1 to be found online at http://informahealthcare.com/doi/abs/10.3109/14397595.2014.990674). Even when the two cases with the highest TLG were excluded from the analysis, the correlation between sIL-2R and TLG was still significant ($P = 0.030$, rs = 0.623).

Table 3. Summary of quantitative data.

| Parameters | |
|---|---|
| MTV (ml) | 51.4 (20.2–92.5) |
| TLG | 154.8 (63.7–324.4) |
| Biomarkers | |
| CRP (mg/dl) | 0.2 (0.1–0.5) |
| LDH (IU/l) | 170 (157–192) |
| sIL-2R (U/ml) | 871.5 (652.5–1337.5) |
| IgG4 (mg/dl) | 736 (539–1150) |

Values are presented as medians (interquartile ranges).
*MTV* metabolic tumor volume, *TLG* total lesion glycolysis, *sIL-2R* soluble interleukin-2 receptor, *IgG4* immunoglobulin G4.

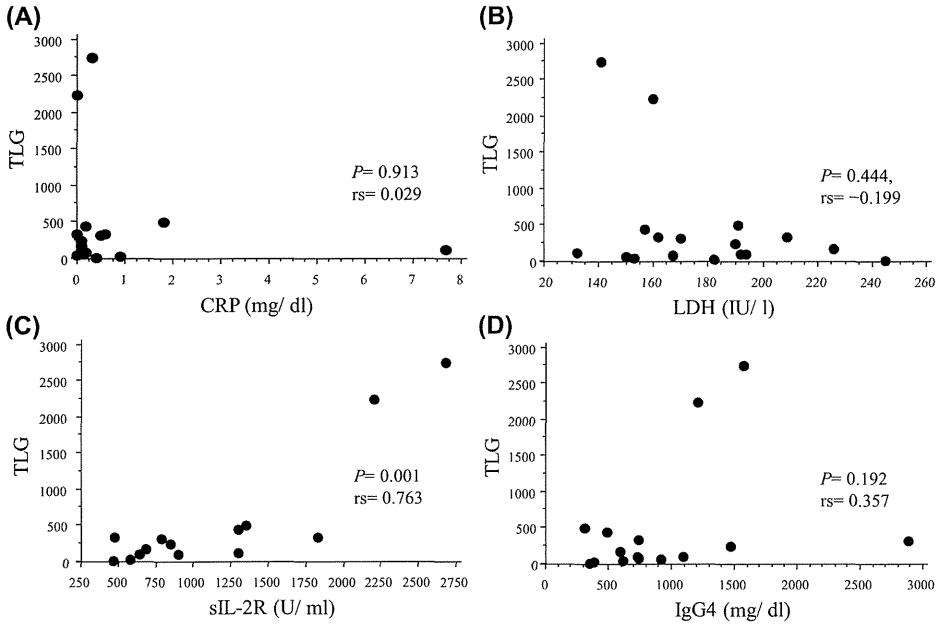


Figure 2. Correlations between TLG and serum biomarker levels. A: CRP, B: LDH, C: sIL-2R, D: IgG4. The serum sIL-2R level correlated significantly with TLG ($P = 0.001$, rs = 0.763), whereas no significant correlations were observed with the other markers. Each graph includes the rs and P values as determined using the Spearman rank correlation coefficient test.

We also performed the same analysis in patients without kidney lesions ($n = 15$). In this analysis, sIL-2R levels also correlated significantly with TLG ($P = 0.020$, rs = 0.717), whereas those of the other markers did not (Supplementary Figure 2 to be found online at http://informahealthcare.com/doi/abs/10.3109/14397595.2014.990674).

### Serial changes in TLG or SUVmax coincident with the clinical course

Follow-up studies were performed in six patients in whom serial changes in TLG FDG-PET/CT were assessed (Table 4 and Supplementary Table 1 to be found online at http://informahealthcare.com/doi/abs/10.3109/14397595.2014.990674). Among these, three cases had received corticosteroid therapy and the others were followed up without therapy. Although intervals between the initial and follow-up studies were not uniform, reductions in TLG were observed in all cases that had received steroid therapy. In contrast, two of the three patients who did not receive steroid therapy showed increases in TLG. When comparing the trends in serial TLG changes with the global disease activity courses, all cases with decreased TLG were considered to have achieved improved global disease activity, whereas all cases with increased TLG were considered to have worsened. On the other hand, in two out of the five patients assessed, the course of SUVmax was not associated with the clinical course.

## Discussion

In this study, we demonstrated that serum sIL-2R levels correlated significantly and positively with TLG. However, no other serum marker levels, including IgG4, correlated significantly with TLG. Serial changes in TLG paralleled clinical disease improvement or worsening. These results indicated the utility of TLG as a marker with which to monitor IgG4-RD activity. To the best of our knowledge, this was the first report to investigate the significance of TLG in IgG4-RD.

In IgG4-RD, although the symptoms are usually mild [14] and resolution is sometimes obtained naturally, as seen in the present study, adequately timed and intense treatment is needed to prevent the irreversible progression of fibrosis [15]. Therefore, evaluations of disease activity are important. However, IgG4-RD affects various organs; therefore, it is difficult to establish an integrated measurement that can evaluate severities of lesions in different organs. To date, several scoring systems have been pro-

Table 4. Serial change of TLG in clinical course.

| | Treatment (+) | | | Treatment (−) | | |
|---|---|---|---|---|---|---|
| | Case 1 | Case 2 | Case 3 | Case 4 | Case 5 | Case 6 |
| Age | 66 | 73 | 77 | 73 | 54 | 53 |
| Gender | Male | Male | Female | Male | Male | Female |
| Affected Organs | Kidney<br>Pancreas | RF<br>SG<br>HMLN | OC<br>Lung<br>HMLN | OC | RF<br>HMLN | Lung<br>Pancreas |
| Test interval (month) | 27 | 1 | 12 | 22 | 18 | 22 |
| Initial dose of corticosteroid* | 40 | 35 | 30 | None | None | None |
| Initial TLG | 86.5 | 154.8 | 324.4 | 11.9 | 108.7 | 0.0 |
| Initial SUVmax | NA | 5.9 | 8.9 | 4.6 | 10.0 | <2.5 |
| Follow-up TLG | 66.9 | 8.0 | 157.6 | 10.6 | 591.5 | 16.8 |
| Follow-up SUVmax | NA | 3.0 | 5.2 | 4.9 | 5.0 | 3.2 |
| Course of global activity | Improved | Improved | Improved | Improved | Worsened | Worsened |

*TLG* total lesion glycolysis, *RF* retroperitoneal fibrosis, *SG* salivary glands, *HMLN* hilar and mediastinal lymph nodes, *OC* ocular cavity

Treatment (+) or (−) indicates whether corticosteroid therapy was initiated or not.

*Recorded when corticosteroid therapy was initiated during the period between initial and follow-up FDG-PET/CT. The corticosteroid dose was adjusted for prednisolone.

posed as tools for evaluating the global disease activity [11,16], but these systems have not been sufficiently established. Moreover, serum IgG4 level was included in the scoring, but in the present study, most of the cases did not undergo follow-up serum IgG4 measurements; therefore, the scoring systems were considered inapplicable. Accordingly, a physician's global assessment was used as a tool for evaluating changes in the disease activity [11,17].

FDG uptake is increased at sites of inflammation [18]. Elevated FDG uptake usually reflects more abundant glucose consumption, thereby indicating accelerated proliferation and increased metabolism [18–20]. Therefore, the degree of FDG uptake is considered to provide information about disease activity [21]. Actually, in some inflammatory diseases such as rheumatoid arthritis or Takayasu aortitis, FDG-PET was reported to have a diagnostic value and function effectively in evaluating treatment response [22–24].

Ebbo et al. performed a qualitative analysis of the FDG-PET/CT scans of IgG4-RD patients. The authors showed increased FDG uptake at the sites of affected lesions and reduced uptake after clinical remission was achieved [4]. Based on these results, they concluded that the FDG-PET/CT findings correlated with the disease activity. However, to date there have been no reports about the quantitative evaluation of FDG-PET/CT for IgG4-RD; therefore, we investigated the clinical significance of TLG in IgG4-RD.

SUVmax is a common and widely used quantitative analysis parameter of PET. This parameter is easily obtained, reproducible, and reader-independent, but it can be influenced by statistical noise. In addition, IgG4-RD patients are likely to have multiple organ involvement and thus multiple lesions. Because TLG is calculated as a summation of SUV of involved areas, we adopted and analyzed TLG as a quantitative value in this investigation.

Regarding the serum biomarkers, we demonstrated in the present study that serum sIL-2R levels strongly correlated with TLG. Although the precise biological role of sIL-2R remains unclear, the serum level of this receptor is considered as an indicator of lymphocyte activation [25] and elevated sIL-2R levels have been reported in several inflammatory diseases such as sarcoidosis [26] and systemic lupus erythematosus [25]. Moreover, elevated serum sIL-2R levels can predict sarcoidosis relapse after therapy [27]. Furthermore, in IgG4-RD, IL-2 is considered to have an important role in lymphocyte activation [28]. Matsubayashi et al. reported elevated serum sIL-2R levels in autoimmune pancreatitis patients and significant reductions in the level of this marker after corticosteroid therapy [29]. Autoimmune pancreatitis is now considered as a pancreatic manifestation of IgG4-RD [1]; therefore, sIL-2R might act as a biomarker of disease activity in IgG4-RD patients. The correlation between TLG and sIL-2R might thus indicate the utility of TLG as a biomarker in IgG4-RD.

In the previous studies, IgG4 is the most intensively investigated biomarker, and its serial changes in its levels were regarded as indicative of treatment responses or reactivation [30]. However, in the present study, IgG4 did not correlate significantly with TLG. The pathophysiological role of IgG4 remains unclear; however, IgG4 secretion is currently believed to occur in response to IL-10 stimulation, which acts to suppress immune responses [31]. Therefore, IgG4 may not directly reflect the intensity of inflammation. This indirect relationship might result in lack of correlation with TLG, although this idea is speculative.

In the analysis of serial FDG-PET/CT studies, all patients who exhibited decreases in TLG showed clinical improvement. On the contrary, two cases with increased TLG exhibited clinical deterioration. This result agreed with the above-described qualitative study [4], and suggested the utility of TLG as a parameter with which to monitor disease activity. On the other hand, in two cases the course of SUVmax was not associated with clinical course (Table 4). In these cases (Case 4 and 5), ocular movement and urinary tract obstruction improved or worsened in parallel with the change in TLG. We assume that the lesion volume might directly affect the function of these organs. In addition, after the treatment, case 2 showed a marked reduction in volume of the affected areas in parallel with TLG (from 154.8 to 8.0), whereas SUVmax showed just a moderate decrease (from 5.9 to 3.0); thus, TLG might exhibit a better association with global activity than SUVmax.

A major disadvantage of FDG-PET/CT is its high cost. Therefore, frequent and regular use of FDG-PET/CT is not possible in daily practice. Given the utility of sIL-2R and IgG4 in disease monitoring, measurement of these biomarkers may be advantageous in terms of cost and convenience compared with FDG-PET/CT. However, levels of both of these biomarkers might be elevated non-specifically because of other diseases or conditions [32,33]. Moreover, it is impossible to obtain site-specific information of activity when multiple lesions exist. In contrast, FDG-PET/CT can evaluate each organ separately [4]; therefore, it is comparatively easier to selectively investigate IgG4-RD lesion activities. For these reasons, serum biomarker evaluation is beneficial in daily practice, whereas more detailed FDG-PET/CT and TLG evaluation is useful as needed. On the other hand, it is still unclear whether comparing a TLG score in different organs has any clinical significance, because even lesions with a low TLG score could significantly aggravate patients (for example, intraorbital space lesions). Given this, further research is needed to better understand this problem.

This study has several limitations. First, this is a retrospective study with existing data deficits including the follow-up data of serum markers. Second, a pathological evaluation was not performed for all estimated lesions; therefore, sites of non-specific inflammation might have been included as IgG4-RD lesions. Third, the number of patients who participated in follow-up FDG-PET/CT studies was small, and intervals between the initial and follow-up FDG-PET/CT studies were not uniform; therefore, it was difficult to perform a statistical analysis regarding changes in TLG. Moreover, given the lack of information about the minimally clinically important difference in TLG, it was difficult to interpret the significance of a small change in TLG as seen in case 4. Fourth, SUV might be influenced by several factors such as the serum glucose level or the interval between the FDG injection and PET emission scan; therefore, the TLG calculations in the present study might exhibit a certain degree of fluctuation. In addition, physiological FDG uptake (such as urine) inevitably influenced TLG values, whereas SUV may show a low level even in the presence of definite lesions (such as interstitial pneumonia) and such lesions were omitted from analysis when SUV was below 2.5. Therefore, in cases where these lesions were present, an accurate evaluation was challenging. Despite these limitations, the present study showed a correlation between TLG and the sIL-2R level, and the serial change of TLG was associated with the clinical course. These findings indicated the utility of TLG for disease monitoring in IgG4-RD. In future studies, validations of these markers using clinically significant outcomes or parameters will be required.

## Acknowledgments

We thank Drs. Y. Imura, M. Hashimoto, R. Nakashima, N. Yukawa, T. Nojima, D. Kawabata, T. Usui, K. Ohmura, and T. Fujii (Department of Rheumatology and Clinical Immunology, Graduate School of Medicine, Kyoto University) for their contributions to clinical practice.

## Conflict of interest

The authors declare no conflict of interests. This study was supported by grants from the respiratory failure research group and the IgG4-related disease research group of the Ministry of Health, Labour and Welfare, Japan. The funding source did not have any role in the study design; in the collection, analysis, and interpretation of data; in the writing of the report; and in the decision to submit the article for publication.

## References

1. Umehara H, Okazaki K, Masaki Y, Kawano M, Yamamoto M, Saeki T, et al. Comprehensive diagnostic criteria for IgG4-related disease (IgG4-RD), 2011. Mod Rheumatol. 2012;22(1):21–30.
2. Deshpande V, Zen Y, Chan JK, Yi EE, Sato Y, Yoshino T, et al. Consensus statement on the pathology of IgG4-related disease. Mod Pathol. 2012;25(9):1181–92.
3. Uchida K, Masamune A, Shimosegawa T, Okazaki K. Prevalence of IgG4-related disease in japan based on nationwide survey in 2009. Int J Rheumatol. 2012;2012:1–5.
4. Ebbo M, Grados A, Guedj E, Gobert D, Colavolpe C, Zaidan M, et al. Usefulness of 2-[18F]-fluoro-2-deoxy-D-glucose-positron emission tomography/computed tomography for staging and evaluation of treatment response in IgG4-related disease: a retrospective multicenter study. Arthritis Care Res (Hoboken). 2014;66(1):86–96.
5. Nakatani K, Nakamoto Y, Togashi K. Utility of FDG PET/CT in IgG4-related systemic disease. Clin Radiol. 2012;67(4):297–305.
6. Larson SM, Erdi Y, Akhurst T, Mazumdar M, Macapinlac HA, Finn RD, et al. Tumor treatment response based on visual and quantitative changes in global tumor glycolysis using PET-FDG imaging. The visual response score and the change in total lesion glycolysis. Clin. Positron Imaging. 1999;2(3):159–71.
7. Lee P, Weerasuriya DK, Lavori PW, Quon A, Hara W, Maxim PG, et al. Metabolic tumor burden predicts for disease progression and death in lung cancer. Int J Radiat Oncol Biol Phys. 2007;69(2):328–33.
8. Chung MK, Jeong HS, Park SG, Jang JY, Son YI, Choi JY, et al. Metabolic tumor volume of [18F]-Fluorodeoxyglucose positron emission tomography/computed tomography predicts short-term outcome to radiotherapy with or without chemotherapy in pharyngeal cancer. Clin Cancer Res. 2009;15:5861–8.
9. Seol YM, Kwon BR, Song MK, Choi YJ, Shin HJ, Chung JS, et al. Measurement of tumor volume by PET to evaluate prognosis in patients with head and neck cancer treated by chemo-radiation therapy. Acta Oncol. 2010;49(2):201–8.
10. Ryu IS, Kim JS, Roh J-L, Cho K-J, Choi S-H, Nam SY, et al. Prognostic significance of preoperative metabolic tumour volume and total lesion glycolysis measured by 18F-FDG PET/CT in squamous cell carcinoma of the oral cavity. Eur J Nucl Med Mol Imaging. 2013;41(3):4521–61.
11. Khosroshahi A, Carruthers MN, Deshpande V, Unizony S, Bloch DB, Stone JH. Rituximab for the treatment of IgG4-related disease. Medicine. 2012;91(1):57–66.
12. Scrucca L, Santucci A, Aversa F. Competing risk analysis using R: an easy guide for clinicians. Bone Marrow Transplant. 2007;40:381–7.
13. EZR_HP. http://www.jichi.ac.jp/saitama-sct/SaitamaHP.files/statmed.html; 2013 Oct pp. 1–1. Report No.: Accessed on 2013 Oct 1.
14. Umehara H, Okazaki K, Masaki Y, Kawano M, Yamamoto M, Saeki T, et al. A novel clinical entity, IgG4-related disease (IgG4RD): general concept and details. Mod Rheumatol. 2012;22(1):1–14.
15. Shimizu Y, Yamamoto M, Naishiro Y, Sudoh G, Ishigami K, Yajima H, et al. Necessity of early intervention for IgG4-related disease–delayed treatment induces fibrosis progression. Rheumatology. 2013;52(4):679–83.
16. Carruthers MN, Stone JH, Deshpande V, Khosroshahi A. Development of an IgG4-RD Responder Index. Int J Rheumatol. 2012;2012:259408.
17. Ebbo M, Daniel L, Pavic M, Sève P, Hamidou M, Andres E, et al. IgG4-related systemic disease: features and treatment response in a French cohort: results of a multicenter registry. Medicine. 2012;91(1):49–56.
18. Signore A, Glaudemans AWJM. The molecular imaging approach to image infections and inflammation by nuclear medicine techniques. Ann Nucl Med. 2011;25(10):681–700.
19. Yamada S, Kubota K, Kubota R, Ido T, Tamahashi N. High accumulation of fluorine-18-fluorodeoxyglucose in turpentine-induced inflammatory tissue. J Nucl Med. 1995;36(7):1301–6.
20. Ishimori T, Saga T, Mamede M, Kobayashi H, Higashi T, Nakamoto Y, et al. Increased 18F-FDG uptake in a model of inflammation: concanavalin A-mediated lymphocyte activation. J Nucl Med. 2002;43:658–63.
21. Weber WA, Schwaiger M, Avril N. Quantitative assessment of tumor metabolism using FDG-PET imaging. Nucl Med Biol. 2000;27(7):683–7.
22. Cheng Y, Lv N, Wang Z, Chen B, Dang A. 18-FDG-PET in assessing disease activity in Takayasu arteritis: a meta-analysis. Clin Exp Rheumatol. 2013;31(1 Suppl 75):S22–7.
23. Wang S-C, Xie Q, Lv W-F. Positron emission tomography/computed tomography imaging and rheumatoid arthritis. Int J Rheum Dis. 2014;17(3):248–55.
24. Santhosh S, Mittal BR, Gayana S, Bhattacharya A, Sharma A, Jain S. F-18 FDG PET/CT in the evaluation of Takayasu arteritis: An experience from the tropics. J Nucl Cardiol. 2014;21(5):993–1000.
25. Smith MF, Hiepe F, Dörner T, Burmester G. Biomarkers as tools for improved diagnostic and therapeutic monitoring in systemic lupus erythematosis. Arthritis Res Ther. 2009;11(6):255.
26. Junghans RP, Waldmann TA. Metabolism of Tac (IL2Ralpha): physiology of cell surface shedding and renal catabolism, and suppression of catabolism by antibody binding. J Exp Med. 1996;183(4):1587–602.
27. Vorselaars ADM, Verwoerd A, Van Moorsel CHM, Keijsers RGM, Rijkers GT, Grutters JC. Prediction of relapse after discontinuation of infliximab therapy in severe sarcoidosis. Eur Respir J. 2014;43:602–9.
28. Okazaki K, Uchida K, Koyabu M, Miyoshi H, Takaoka M. Recent advances in the concept and diagnosis of autoimmune pancreatitis and IgG4-related disease. J Gastroenterol. 2011;46:277–88.
29. Matsubayashi H, Uesaka K, Kanemoto H, Asakura K, Kakushima N, Tanaka M, et al. Soluble IL-2 receptor, a new marker for autoimmune pancreatitis. Pancreas. 2012;41(3):493–6.
30. Tabata T, Kamisawa T, Takuma K, Egawa N, Setoguchi K, Tsuruta K, et al. Serial changes of elevated serum IgG4 levels in IgG4-related systemic disease. Intern Med. 2011;50(2):69–75.
31. Zen Y, Nakanuma Y. IgG4-related disease: a cross-sectional study of 114 cases. Am. J Surg Pathol. 2010;34(12):1812–9.
32. Yamamoto M, Tabeya T, Naishiro Y, Yajima H, Ishigami K, Shimizu Y, et al. Value of serum IgG4 in the diagnosis of IgG4-related disease and in differentiation from rheumatic diseases and other diseases. Mod Rheumatol. 2011;22(3):419–25.
33. Ryuko H, Otsuka F. A comprehensive analysis of 174 febrile patients admitted to Okayama University Hospital. Acta Med Okayama. 2013;67(4):227–37.

## Supplementary material available online

Supplementary Figures 1, 2 and Table 1.

Contents lists available at ScienceDirect

Respiratory Investigation

journal homepage: www.elsevier.com/locate/resinv

Short Communication

# Proposed diagnostic criteria for IgG4-related respiratory disease ☆

*Shoko Matsui*[a,*], *Hiroshi Yamamoto*[b], *Seijiro Minamoto*[c], *Yuko Waseda*[d], *Michiaki Mishima*[e], *Keishi Kubo*[f]

[a]*Health Administration Center, University of Toyama, Gofuku 3190, Toyama-shi, Toyama 930-8555, Japan*
[b]*Shinshu University School of Medicine, Japan*
[c]*Osaka Prefectural Medical Center for Respiratory and Allergic Diseases, Japan*
[d]*Kanazawa University Graduate School of Medical Science, Japan*
[e]*Graduate School of Medicine, Kyoto University, Japan*
[f]*Nagano Prefectural Hospital Organization, Japan*

ARTICLE INFO

*Article history:*
Received 17 March 2015
Received in revised form
7 September 2015
Accepted 11 September 2015

## 1. Background on the preparation of the diagnostic criteria

IgG4-related disease (IgG4-RD) [1] is a newly recognized systemic disease characterized by an elevated serum level of IgG4, infiltration of IgG4-positive plasma cells into affected lesions, and fibrosis. In 2011, comprehensive diagnostic criteria for IgG4-RD were proposed by the Study Group of Intractable Diseases from the Ministry of Health, Labor and Welfare, Japan (MHLW) [2], and these criteria have been gaining increasing acceptance.

The comprehensive diagnostic criteria [2] are highly convenient for diagnosing IgG4-RD and are based on findings common to multiple organs. However, because the field of medicine has become increasingly specialized and subdivided, the Study Group at the MHLW has recognized the need for organ-specific diagnostic criteria focusing on the specific features of lesions in individual organs; organ-specific diagnostic criteria for the pancreas, kidney, and other sites of involvement have already been published [3,4].

Following the release of the comprehensive diagnostic criteria for IgG4-RD 2011 [2], an attempt was made by the subcommittee on IgG4-RD supported by the MHLW to prepare similar diagnostic criteria for lesions arising in the respiratory organs. The criteria for the respiratory organs were presented at a symposium at the 54th Annual Meeting of the Japanese Respiratory Society (2014), where the final diagnostic criteria

☆This paper was previously peer-reviewed and published by the Journal of the Japanese Respiratory Society [7].

*Corresponding author. Tel.: +81 76 445 6911; fax: +81 76 445 6908.
E-mail addresses: smatsui@med.u-toyama.ac.jp (S. Matsui), yama5252@shinshu-u.ac.jp (H. Yamamoto), minamotos@ra.opho.jp (S. Minamoto), yuwaseda@gmail.com (Y. Waseda), mishima@kuhp.kyoto-u.ac.jp (M. Mishima), kubo-keishi@pref-nagano-hosp.jp (K. Kubo).

http://dx.doi.org/10.1016/j.resinv.2015.09.002


Please cite this article as: Matsui S, et al. Proposed diagnostic criteria for IgG4-related respiratory disease. Respiratory Investigation (2015), http://dx.doi.org/10.1016/j.resinv.2015.09.002

**Table 1 – Diagnostic criteria for IgG4-related respiratory disease.**

A. Diagnostic factors

I. Chest imaging

Imaging findings include any of the following intrathoracic lesions, such as hilar/mediastinal lymphadenopathy, bronchial wall/bronchovascular bundle thickening, interlobular septal wall thickening, nodular shadow, infiltrative shadow, pleural thickening and/or effusion.

II. Serology

Elevated serum IgG4 concentration of ≥ 135 mg/dl

III. Histology

Two or more of the following items are required from intrathoracic organ tissues.

a: ≥ 3 Items; b: 2 items

(1) Marked lymphoplasmacytic cell infiltration into interstitium of peribronchovascular sheath, interlobular septal wall, and/or pleura.

(2) IgG4/IgG-positive cell ratio >40% and/or >10 IgG4-positive cells/high power field.

(3) Obliterative phlebitis or obliterative arteritis.

(4) Storiform fibrosis or fibrosis consisting of proliferating spindle-shaped cells around infiltrating lymphocytes.

IV. Other organ involvement

The presence of lesions in the extrathoracic organs satisfying the diagnostic criteria of IgG4-related disease such as sclerosing dacryoadenitis/sialadenitis, autoimmune pancreatitis, IgG4-related sclerosing cholangitis, IgG4-related kidney disease, and retroperitoneal fibrosis.

V. Reference finding

Hypocomplementemia

B. Diagnosis

1. Definite diagnosis (definite): I+II+IIIa, or I+II+IIIb+IV
Histological definite diagnosis [definite (histological)]: I+all four items of III
2. Probable diagnosis (probable): I+II+IV, or I+II +IIIb+V
3. Possible diagnosis (possible): I+II+IIIb

C. Differential diagnosis

It is important to differentiate IgG4-related respiratory disease from the following diseases with similar features.

Castleman disease (plasma cell type), collagen-disease-related lung disease, granulomatosis with polyangiitis (Wegener granuloma), eosinophilic granulomatosis with polyangiitis (Churg–Strauss syndrome), sarcoidosis, respiratory organs infection, Rosai–Dorfman disease, inflammatory myofibroblastic tumor, malignant lymphoma, lung cancer.

**Table 2 – Diagnostic criteria of IgG4 -related respiratory disease: appendix for Table 1.**

1. Imaging findings

- Hilar/mediastinal lymphadenopathy and bronchial wall/bronchovascular thickening are frequent findings.
- Lesions are found predominantly in the interstitium including the interlobular septa and pleura.
- Sometimes detected as an intrathoracic nodular, mass or infiltrative shadow.
- Since the imaging findings are non-specific, conditions noted in the Differential diagnosis, especially infection and malignancy, must be ruled out.

2. Clinical/test findings

- Presence or history of allergic conditions such as allergic rhinitis and bronchial asthma is sometimes noted.
- Hyper-IgG-emia, hyper-IgE-emia are frequently associated, while simultaneous elevation of serum IgA and IgM is rare.
- Antinuclear antibodies and/or rheumatoid factor positivity, and hypocomplementemia are sometimes found.
- No or only very mild findings of inflammation such as leukocytosis and CRP elevation.

3. Pathological findings

- Presence of fibrotic foci associated with marked lymphoplasmacytic cell infiltration into the tissues such as interstitium of peribronchovascular sheath, interlobular septal wall, pleura and contiguous alveolar septal wall.
- 'Storiform fibrosis' is the type of fibrosis typically seen, and consists of proliferating spindle-shaped cells associated with lymphoplasmacytic cell infiltration. The arrangement of these components is irregular and sometimes assumes a whirlpool-like pattern.
- Formation of mass lesions that appear to bury the alveolar spaces is sometimes observed because of the presence of marked cellular infiltration and fibrosis.
- Scattered eosinophil infiltrates are occasionally found, while neutrophil infiltrates and granulomas are usually not.
- For the pathological diagnosis, use of surgical biopsy specimens is desirable.

4. Extra-thoracic organ lesions

- Extra-thoracic organ lesions are those that satisfy the established organ-specific diagnostic criteria (pancreas, bile duct, or kidney), or pathological findings such as prominent IgG4-positive lymphoplasmacytic cell infiltration and fibrosis consistent with the characteristic (organ-specific) clinical and imaging findings (lacrimal gland, salivary gland, or retroperitoneum).

were prepared after discussion and agreement by all members present. In this report, we outline these criteria.

## 2. Guidelines for IgG4-related respiratory disease

### 2.1. *Nomenclature of respiratory tract lesions*

At the International Symposium on IgG4-RD held in Boston in 2011, two separate names were adopted for the respiratory tract lesions of IgG4-related disease: 'IgG4-related lung disease' and 'IgG4-related pleural disease' [5]. However, since a subsequent report that respiratory tract lesions are typically interstitial lesions [6], the Ministry of Health group decided to refer to lesions of both the intrathoracic respiratory organs and auxiliary structures collectively as 'IgG4-related respiratory disease (IgG4-RRD)'.

### 2.2. *The diagnostic criteria for IgG4-RRD*

The diagnostic criteria for IgG4-RRD are listed in Table 1. Some commentary has been added (Table 2) to enhance the understanding of chest imaging, clinical/laboratory results, and pathological findings of these diagnostic criteria. An algorithm has also been prepared to concretely illustrate the process whereby the diagnosis is reached (Fig. 1).

## 3. Summary

The diagnostic criteria of IgG4-RRD are outlined. We hope for further consideration and acceptance of the criteria.

Please cite this article as: Matsui S, et al. Proposed diagnostic criteria for IgG4-related respiratory disease. Respiratory Investigation (2015), http://dx.doi.org/10.1016/j.resinv.2015.09.002